Temperature dependent phonon evolutions and optical properties of highly c-axis oriented CuGaO2 semiconductor films grown by the sol-gel method

M. J. Han, K. Jiang, J. Z. Zhang, Y. W. Li, Z. G. Hu et al.

Citation: Appl. Phys. Lett. **99**, 131104 (2011); doi: 10.1063/1.3641477
View online: http://dx.doi.org/10.1063/1.3641477
View Table of Contents: http://apl.aip.org/resource/1/APPLAB/v99/i13
Published by the American Institute of Physics.

Temperature dependent phonon evolutions and optical properties of highly *c*-axis oriented $CuGaO_2$ semiconductor films grown by the sol-gel method

M. J. Han (韩美杰), K. Jiang (姜凯), J. Z. Zhang (张金中), Y. W. Li (李亚巍), Z. G. Hu (胡志高),[a)]
and J. H. Chu (褚君浩)
Key Laboratory of Polar Materials and Devices, Ministry of Education, Department of Electronic Engineering, East China Normal University, Shanghai 200241, People's Republic of China

(Received 2 August 2011; accepted 30 August 2011; published online 26 September 2011)

Transparent conductive $CuGaO_2$ oxide films were prepared on sapphire substrates by the sol-gel method. The highly *c*-axis orientation and optical transparency (60%-80%) in the visible region were obtained. It indicates that the A_{1g} phonon mode shifts about 20 cm^{-1} with the temperature due to the thermal expansion of the lattice and anharmonic phonon coupling. Moreover, temperature-dependent dielectric function has been investigated and three electronic transitions located at about 1.05, 2.67, and 3.99 eV can be uniquely assigned. It was found that the optical band gap of the $CuGaO_2$ film decreases with the temperature, which mainly originated from the electron-phonon interactions. © *2011 American Institute of Physics*. [doi:10.1063/1.3641477]

Transparent conductive oxides (TCOs) have been attracted much attention because of their functional combination of transparency and electrical conductivity.[1–4] And the interest of delafossite family as stable *p*-type wide band transparent semiconductors has been increased since *p*-type $CuAlO_2$ films have been fabricated.[5] The delafossite structure $CuMO_2$ (M = Al, Ga, and In) can be visualized as consisting of two alternate layers: a planar layer of Cu cation in a triangular pattern and a layer of edge-sharing MO_6 octahedra flattened with respect to the *c*-axis.[5,6] Although most delafossite films have been prepared by vacuum based technologies,[7–10] there are only a few reports on the sol-gel synthesis of *p*-type $CuGaO_2$ films. This is because the preparation of $CuGaO_2$ film is more difficult than that of $CuAlO_2$ film due to evaluation of thermodynamic and kinetic stabilities.[11] Note that the diverse optical band gap (OBG) of $CuGaO_2$ films at room temperature (RT) has been reported by different groups.[7,12,13] Nevertheless, the intrinsic mechanisms of the optical response and its temperature evolution have not been addressed up to now. Moreover, the nature of the indirect and direct band gap in $CuGaO_2$ materials is still not well understood.[14] In this letter, the microstructure, phonon modes, and electronic band structures of $CuGaO_2$ epitaxial films at different temperature ranges have been systematically discussed.

Gallium nitrate hydrate [$Ga(NO_3)_3 \cdot 5.97H_2O$, 99.9%, 1.4552 g] was dissolved in anhydrous ethanol (C_2H_6O, 99.7%, 20 ml) with magnetic stirring. After the solution was stable and became transparent and homogeneous, copper (II) acetate hydrate [$Cu(AcO)_2 \cdot H_2O$, 99%, 0.7985 g] was added into the solution. Stirring was continuous until copper acetate was completely dissolved. Then a little of ethanolamine (C_2H_7NO, 99%) as additive was added into the mixed solution. The cleaned precursors were spin-coated onto (001) sapphire substrates at a speed of 4000 rpm for 20 s. The deposited films were preheated at 300 °C for 5 min in air to evaporate the solvent and remove organic residues in a rapid thermal processing. Finally, the films were annealed at 900 °C for 30 min in N_2 with a flow of 2.5 l/min.

The crystallization, surface morphology, and cross-section microstructure of the $CuGaO_2$ film were characterized using x-ray diffraction (XRD, D/MAX-2550 V, Rigaku Co.), atomic force microscopy (AFM, Digital Instruments Dimension 3100, Veeco), and scanning electron microscope (SEM, S-3000N, Philips XL30FEG). Raman scattering experiments were carried out by a micro-Raman spectrometer (Jobin-Yvon LabRAM HR 800 UV) at 85-873 K and the 325 nm laser line was applied as the exciting source. The temperature-dependent transmittance spectra were recorded by a double beam ultraviolet-infrared spectrophotometer (PerkinElmer UV/VIS Lambda 950) at the photon energy of 2650-190 nm (0.5-6.5 eV). The sample was mounted on a cold stage of an optical cryostat (Janis SHI-4-1) and capable of cooling from 300 to 8 K.

Fig. 1(a) shows the XRD pattern of the $CuGaO_2$ film and no impurity phase is observed. As can be seen, the appearance of only (00*l*) diffraction peaks indicates that the film is preferentially oriented along the *c*-axis perpendicular to the substrate surface. The full width at half-maximum (FWHM) of the (006) peak is about 0.198°, suggesting good crystallinity of the film. From the FWHM of the (006) peak, the crystallite size of the samples is 48.2 nm estimated by the Scherrer formula [$D = 0.9\lambda/(\beta \cos \theta)$]. Moreover, the lattice parameters $a = 2.931$ Å and $c = 17.151$ Å were determined for the epitaxial $CuGaO_2$ film, which are slightly less than those ($a = 2.977$ Å and $c = 17.171$ Å) of bulk ceramic.[6] It should be noted that the (001) sapphire substrate induced the *c*-axis orientation $CuGaO_2$ film. It may be due to the heteroepitaxial relationship $(001)_{CuGaO_2} \| (001)_{Al_2O_3}$ between the $CuGaO_2$ film and sapphire substrate, because both $CuGaO_2$ and sapphire have closest-packed layers of oxygen ions orientated perpendicular to the *c*-axis.[7] Fig. 1(b) shows each grain of the $CuGaO_2$ film is closely packed and the root-mean-square roughness of the surface is 4.78 nm, which is approximately 2.39% of the film thickness. From the cross-sectional structure of the $CuGaO_2$ film [Fig. 1(c)], the thickness is estimated to be about 200 nm.

[a)]Author to whom correspondence should be addressed. Electronic mail: zghu@ee.ecnu.edu.cn. Tel.: +86-21-54345150. FAX: +86-21-54345119.

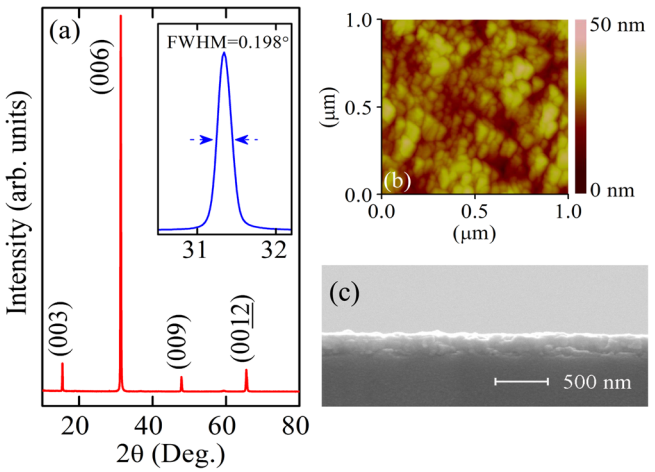

FIG. 1. (Color online) (a) The XRD pattern of the $CuGaO_2$ film on the *c*-plane sapphire substrate, and the inset shows the FWHM of the (006) diffraction peak, (b) AFM surface morphology, and (c) cross-sectional SEM image of the $CuGaO_2$ film.

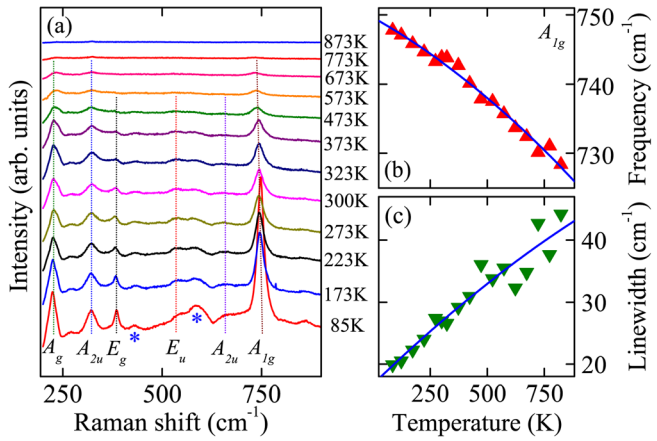

FIG. 2. (Color online) (a) Raman spectra of the $CuGaO_2$ film recorded at different temperatures from 85 to 873 K. Note that the label "*" indicates the substrate's phonon modes. The temperature dependent of (b) frequency and (c) FWHM of the experimental data (dot lines) and the corresponding theoretical fitting (solid lines) for the A_{1g} phonon mode.

Fig. 2(a) shows Raman spectra of the $CuGaO_2$ film. According to group theory, a general mode at the Brillouin zone center as $\Gamma = A_{1g} + E_g + 3A_{2u} + 3E_u$, out of which A_{1g} and E_g symmetry are Raman active.[6,15,16] The phonon characteristics of the $CuGaO_2$ film became weaker and broader with increasing the temperature. The A_{1g} phonon mode disappears abruptly and the Raman spectra almost present a straight line at 873 K. It can be inferred that the transition above 823 K is associated with the lattice relaxation along the *c*-axis and results in the structural phase transition. In order to account for the frequencies of the A_{1g} phonon mode at different temperatures, the damped harmonic oscillator model was used to fit the A_{1g} Raman profile. The results of the frequency shift and linewidth with the temperature are presented in Figs. 2(b) and 2(c), respectively. A continuous decrease in the A_{1g} peak frequency with the temperature was clearly seen, which can be explained by the perturbation model. The model can be written as $\omega(T) = \omega_0 + \Delta\omega_1(T) + \Delta\omega_2(T)$, where ω_0 is the intrinsic harmonic frequency of the optical mode, $\Delta\omega_1(T)$ is the thermal-expansion contribution to the frequency, and $\Delta\omega_2(T)$ is the contribution due to cubic, quadratic, and higher order anharmonic coupling of phonons. The lattice expansion can be explained by the following equation: $\Delta\omega_1(T) = \omega_0[\exp[-\gamma\int_0^T[\alpha_c(T) + 2\alpha_a(T)]dT] - 1]$, the Grüneisen parameter of the A_{1g} phonon mode in the $CuGaO_2$ film with $\gamma = 1.3$, α_a and α_c are the linear coefficients of thermal expansion corresponding to the *a* and *c* axes with $\alpha_a = 11.0 \times 10^{-6}$, $\alpha_c = 4.1 \times 10^{-6}$.[6,15,17] The term related to anharmonic optical phonon coupling can be written as $\Delta\omega_2(T) = A\left[1 + \frac{2}{e^x-1}\right] + B\left[1 + \frac{3}{e^y-1} + \frac{3}{(e^y-1)^2}\right]$. The temperature dependent linewidth can be written as $\Gamma(T) = \Gamma_0 + \Gamma_2$, $\Gamma_2 = C\left[1 + \frac{2}{e^x-1}\right] + D\left[1 + \frac{3}{e^y-1} + \frac{3}{(e^y-1)^2}\right]$. Note that the first term corresponds to three phonon process (two phonon decaying), and the second term corresponds to four phonon process (three phonon decaying).[16,18] The best-fit values of anharmonic constants for the A_{1g} phonon mode in the $CuGaO_2$ film are $\omega_0 = 749.6\ cm^{-1}$, $A = 9.95 \times 10^{-12}\ cm^{-1}$, $B = -1.15 \times 10^{-23}\ cm^{-1}$, $\Gamma = 16.8\ cm^{-1}$, $C = 5.13 \times 10^{-11}\ cm^{-1}$, $D = -8.2 \times 10^{-24}\ cm^{-1}$, respectively. It suggests that the frequency shift and linewidth for the A_{1g} phonon mode can be mainly due to the thermal expansion of the lattice and the three phonon anharmonic coupling process.

An enlarged spectral region near the absorption edge (3.5-3.8 eV) is plotted in Fig. 3(a). The absorption edge shows a blueshift trend with decreasing the temperature, and the $CuGaO_2$ material has a negative temperature coefficient. As shown in Fig. 3(b), the $CuGaO_2$ film is transparent, having an optical transmittance of 60%-80% in the whole visible range. A three-phase layered structure (air/film/substrate) is applied to simulate the transmittance spectra of the $CuGaO_2$ film. The optical response of the $CuGaO_2$ film can be expressed using three Tauc-Lorentz (TL) oscillator function.[19] For example, the TL parameter values of the $CuGaO_2$ film at 8, 150, and 300 K is listed in Table I. As can be seen, three optical transition peaks at RT are located at 1.05, 2.67, and 3.99 eV, respectively. With regards to the valence band, at the Γ-point, the Cu 3*d* states form the top of the valence band; Cu $3d(z^2)$ states strongly mix with O $2p_z$ states giving rise to two bonding states deep in the valence band and one antibonding state which is the lowest conduction band at Γ. In lower symmetry directions, Cu 3*d* bands strongly mix with O $2p_{xy}$ states and they disperse upwards, due to *p-d* repulsion, attaining a maximum at the L- or F-points.[12,13,20] Based on the theoretical calculations and experimental observations, the $TL_{(j=1,2,3)}$ oscillators can be uniquely assigned to the following electronic transitions: (1) the indirect fundamental band transition between the valence band maximum on the Γ-F line near F of the rhombohedral Brillouin zone and the conduction band minimum at Γ, (2) the direct band transition at Γ of the rhombohedral Brillouin zone, and (3) the direct band transition at F (L) with charge densities in the interstitial region, respectively. Note that the transition peaks shift towards the higher energy side with decreasing the temperature. This is because the electronic orbital hybridization, band splitting, and atom interaction can be strongly affected by the temperature, which results in the modification of electronic band structures. In addition, the phenomena are also related to the electron-phonon interaction and the lattice thermal expansion with the temperature.

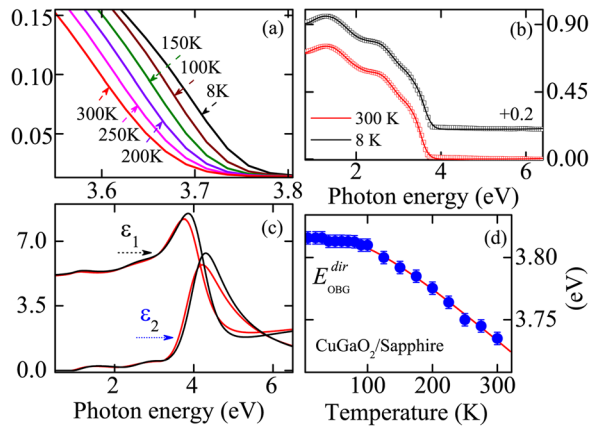

FIG. 3. (Color online) (a) Transmittance spectra of the $CuGaO_2$ film with different temperature, (b) the experimental (dotted curves) and fitting (solid curves) transmittance spectra at 8 and 300 K, (c) real (ε_1) and imaginary (ε_2) parts of the dielectric constants of the $CuGaO_2$ film at 8 and 300 K, and (d) the temperature dependence of the OBG (dot curve) and Bose-Einstein model fitting result (solid curve).

Interestingly, the direct transitions from the TL_2 and TL_3 oscillators are more striking compared with the indirect transition, which result in the fact that the $CuGaO_2$ film is transparent in the visible region.

The evaluated dielectric function $\tilde{\varepsilon} = \varepsilon_1 + i\varepsilon_2$ of the $CuGaO_2$ film at 8 and 300 K is shown in Fig. 3(c). The maximum position of dielectric function has a redshift trend with increasing the temperature. Fig. 3(d) shows the temperature dependence of the OBG energy for the $CuGaO_2$ film. The direct transitions are the dominant effect here, which is consistent with the experimental results. The power law behavior of Tauc $(\alpha E)^2 \propto (E - E_{OBG}^{dir})$ is for allowed direct transition and E_{OBG}^{dir} is the OBG.[21,22] From Fig. 3(d), it can be found that the E_{OBG}^{dir} value decreases from 3.815 to 3.735 eV, corresponding to increase in the temperature from 8 to 300 K. Generally, the temperature dependence of the E_{OBG}^{dir} parameter can be described using the Bose-Einstein model, in which the carrier-phonon coupling is taken into account and can be written as $E_{OBG}(T) = E_{OBG}(0) - 2a_B/[\exp(\Theta_B/T) - 1]$.[23] The $E_{OBG}(0)$ value is estimated to be about 3.815 eV, the parameters a_B and Θ_B are 68.9 meV and 296.2 K, respectively. It is widely recognized that the electron-phonon interaction and lattice thermal expansion are responsible for the OBG shrinkage with the temperature. In particular, the electron-phonon interaction, which includes the contributions from both acoustic as well as optical phonons, is usually the dominating one. With increasing the temperature, the longitudinal phonons change the interatomic distance along the direction of their propagation and the transversal modes were perpendicular to their propagation.[21,24] Therefore, the variation in the lattice constant, due to the dilatation of lattice and the shortening of interatomic distances, can result in the modification of electronic band structure, which further move the conduction band downward and the valence band upward.

TABLE I. The Tauc-Lorentz parameter values of the $CuGaO_2$ film are determined from the simulation of transmittance spectra at 8, 150, 300K. Note that A_j, E_{pj}, Γ_j, and E_{oj} are the amplitude, peak position energy, broadening term, and Tauc gap energy of the oscillator, respectively.

Temperature (K)	ε_∞	Oscillator (TL_j)	A_j (eV)	E_{pj} (eV)	Γ_j (eV)	E_{oj} (eV)
8	3.32	$j=1$	3.33	1.16	1.20	0.94
		$j=2$	9.48	2.71	1.50	2.12
		$j=3$	103	4.13	1.09	3.14
150	3.28	$j=1$	3.40	1.13	1.19	0.93
		$j=2$	9.26	2.70	1.56	2.10
		$j=3$	111	4.08	1.08	3.14
300	3.30	$j=1$	3.27	1.05	1.16	0.88
		$j=2$	8.89	2.67	2.02	1.98
		$j=3$	112	3.99	1.14	3.13

In summary, we prepared (00*l*) preferred orientation and well crystallized $CuGaO_2$ films by the sol-gel method. The microstructure, phonon modes, and electronic band structures at different temperature ranges have been investigated.

This work was financially supported by projects: Grant Nos. 60906046, 11074076, 2007CB924901, 2011CB922200, NCET-08-0192, PCSIRT, 10DJ1400201, 10SG28, 10ZR1409800, 09ZZ42, and The Program for Professor of Special Appointment (Eastern Scholar) at Shanghai Institutions of Higher Learning.

[1] J. F. Li, L. B. Hu, J. Liu, L. Wang, T. J. Marks, and G. Grüner, Appl. Phys. Lett. **93**, 083306 (2008).
[2] Y. M. Kim, W. J. Lee, D.-R. Jung, J. M. Kim, S. H. Nam, H. C. Kim, and B. W. Park, Appl. Phys. Lett. **96**, 171902 (2010).
[3] Z. Y. Hu, J. J. Zhang, Z. H. Hao, Q. Y. Hao, X. H. Geng, and Y. Zhao, Appl. Phys. Lett. **98**, 123302 (2011).
[4] H. M. Luo, M. K. Jain, T. M. McCleskey, E. Bauer, A. K. Burrell, and Q. X. Jia, Adv. Mater. **19**, 3604 (2007).
[5] H. Kawazoe, M. Yasukawa, H. Hyodo, M. Kurita, H. Yanagi, and H. Hosono, Nature **389**, 939 (1997).
[6] J. Pellicer-Porres, A. Segura, E. Martínez, A. M. Saitta, A. Polian, J. C. Chervin, and B. Canny, Phys. Rev. B **72**, 064301 (2005).
[7] K. Ueda, T. Hase, H. Yanagi, H. Kawazoe, H. Hosono, H. Ohta, M. Orita, and M. Hirano, J. Appl. Phys. **89**, 1790 (2001).
[8] R. S. Yu, S. C. Liang, C. J. Lu, D. C. Tasi, and F. S. Shieu, Appl. Phys. Lett. **90**, 191117 (2007).
[9] Th. Dittrich, L. Dloczik, T. Guminskaya, M. Ch. Lux-Steiner, N. Grigorieva, and I. Urban, Appl. Phys. Lett. **85**, 742 (2004).
[10] T. Mine, H. Yanagi, K. Nomura, T. Kamiya, M. Hirano, and H. Hosono, Thin Solid Films **516**, 5790 (2008).
[11] K. Yuh, H. Motohiro, K. Yuhki, E. Satoshi, O. Eri, and H. Takuya, J. Therm. Anal. Calorim. **99**, 57 (2010).
[12] X. L. Nie, S.-H. Wei, and S. B. Zhang, Phys. Rev. Lett. **88**, 066405 (2002).
[13] M. N. Huda, Y. Yan, A. Walsh, S.-H. Wei, and M. M. Al-Jassim, Phys. Rev. B **80**, 035205 (2009).
[14] J. Pellicer-Porres, A. Segura, A. S. Gilliland, A. Muñoz, P. Rodríguez-Hernández, D. Kim, M. S. Lee, and T. Y. Kim, Appl. Phys. Lett. **88**, 181904 (2006).
[15] J. Pellicer-Porres, D. Martínez-Garía, A. Segura, P. Rodríguez-Hernández, A. Muñoz, J. C. Chervin, N. Garro, and D. Kim, Phys. Rev. B **74**, 184301 (2006).
[16] S. P. Pavunny, A. Kumar, and R. S. Katiyar, J. Appl. Phys. **107**, 013522 (2010).
[17] T. Ishiguro, N. Ishizawa, N. Mizutani, and M. Kato, J. Solid State Chem. **41**, 132 (1982).
[18] M. Balkanski, R. F. Wallis, and E. Haro, Phys. Rev. B **28**, 1928 (1983).
[19] G. E. Jellison, Jr. and F. A. Modine, Appl. Phys. Lett. **69**, 371 (1996); **69**, 2137 (1996).
[20] S. Gilliland, J. Pellicer-Porres, A. Segura, A. Muñoz, P. Rodríguez-Hernández, D. Kim, M. S. Lee, and T. Y. Kim, Phys. Status Solidi B **244**, 309 (2007).
[21] W. W. Li, J. J. Zhu, J. D. Wu, J. Gan, Z. G. Hu, M. Zhu, and J. H. Chu, Appl. Phys. Lett. **97**, 121102 (2010).
[22] Z. G. Hu, Y. W. Li, J. D. Wu, J. Sun, Q. W. Shu, X. X. Zhong, Z. Q. Zhu, and J. H. Chu, Appl. Phys. Lett. **93**, 181910 (2008).
[23] M. Beaudoin, A. J. G. DeVries, S. R. Johnson, H. Laman, and T. Tiedje, Appl. Phys. Lett. **70**, 3540 (1997).
[24] S. Biernacki, U. Scherz, and B. K. Meyer, Phys. Rev. B **49**, 4501 (1994).